Modeling 3D Crustal Velocities in the Vicinities of Alaska and the Bering Sea

Richard A. Snay, (retired) NOAA's National Geodetic Survey, 427 Homewood Circle, Frederick, Maryland, U.S.A., 21702

Jeffrey T. Freymueller, Department of Earth and Environmental Sciences, Michigan State University, East Lansing, Michigan, U.S.A., 48824

Michael L. Dennis, NOAA's National Geodetic Survey, 1315 East-West Highway, Silver Spring, Maryland, U.S.A., 20910

Key Points:

- TRANS4D enables its users to transform 3D positional coordinates across time and among several popular terrestrial reference frames
- TRANS4D has been enhanced to include new 3D crustal velocity models for the vicinities of Alaska and the Bering Sea
- Evidence is provided for the existence of a Bering tectonic plate and for part of the boundary between this plate and the North American plate

Abstract

This document introduces Version 0.4 of the TRANS4D software, where TRANS4D is short for *Transformations in Four Dimensions*. TRANS4D enables geospatial professionals and others to transform three-dimensional positional coordinates across time and among several popular terrestrial reference frames. Version 0.4 introduces new crustal velocity models for the vicinities of Alaska and the Bering Sea, including parts of northwestern Canada and eastern Russia. These new models supplement existing velocity models for the continental United States as well as for most of Canada and for a neighborhood of the Caribbean plate. This document also provides evidence for the existence of a Bering tectonic plate, and it presents estimates for the Euler-pole parameters of this hypothesized plate. Moreover, estimated horizontal velocities computed at several geodetic stations located in Alaska provide evidence for the existence of part of the plate boundary separating the North American plate and the hypothesized Bering plate.

Key Words: transforming 3-D positional coordinate across time, tectonic deformation, glacial isostatic deformation

1. Introduction

In 2016, [1] introduced numerical models that quantify three-dimensional (3D) crustal velocities as a function of latitude and longitude for the conterminous United States (CONUS) and for most of Alaska and Canada. These models provide the foundation for Version 0.1 of the TRANS4D software, where TRANS4D is short for *Transformations in Four Dimensions*. TRANS4D is being developed to enable geospatial professionals and others to apply estimated velocities when transforming 3D positional coordinates referred to one date to corresponding 3D positional coordinates referred to an alternative date. Moreover, users can apply TRANS4D to transform positional coordinates from one terrestrial reference frame to another for a suite of popular reference frames, including all reference frames of the International Terrestrial Reference System up to and including the recently released ITRF2020 reference frame [2], plus all existing reference frames of the International Global Navigation Satellite System

Service up to and including IGS20, and all reference frames of the World Geodetic System of 1984 up to and including WGS_84(G1762), as well as three regional reference frames of the North American Datum of 1983 (referred to the North America plate, the Pacific plate, and the Mariana plate, respectively). TRANS4D also addresses changes in positional coordinates due to phenomena other than constant velocities. In particular, TRANS4D contains models quantifying the coseismic displacements associated with 33 North American earthquakes (of which four occurred in Alaska), and a model for the postseismic motion associated with the M7.9 Denali Fault earthquake that occurred in central Alaska on November 3, 2002. This document, however, will address only the particular crustal motion associated with constant velocities.

TRANS4D's velocity models include a collection of two-dimensional (2D) grids (in latitude and longitude) where each grid spans a specified spherical rectangle, and where an estimated 3D velocity (north, east, up components) is recorded for each grid node, together with the three standard deviations associated with these three velocity components. For each point located within the span of a given rectangular grid, TRANS4D employs bilinear interpolation to estimate the point's 3D velocity and its associated three standard deviations from corresponding values stored at the four nodes that define the grid cell encompassing the location of interest.

The velocity models encoded in TRANS4D have been derived from repeated geodetic observations—primarily GNSS observation—but leveling, trilateration, and other geodetic data types have also been employed. Thanks to the rapid increase in the number of continuously operating GNSS stations distributed around the world, velocity models can be upgraded relatively frequently. Accordingly, Version 0.2 of TRANS4D [3] provided a much-improved velocity model for that part of CONUS located west of longitude 107° W. The more accurate velocities residing in Version 0.2 benefitted from the use of an improved velocity-interpolation algorithm compared to that used for Version 0.1, as well as longer observational histories at many of the stations involved in Version 0.1. Also, Version 0.2 benefitted from the existence of estimated velocities at many additional geodetic stations. Version 0.3 [4] expanded TRANS4D's scope to include 3D crustal velocity estimates for a neighborhood of the Caribbean plate.

This document introduces Version 0.4 of the TRANS4D software. In particular, it introduces 3D crustal velocity models for areas encompassing Alaska and the Bering Sea. As presented in Figure 1, the new velocity models include two distinct regions each spanned by separate spherical rectangles. In this document, the rectangle to the east is referred to as the "Alaska region", and the rectangle to the west is referred to as the "Bering region". The area of the Alaska region ranges between latitudes 53°N and 72°N and between longitudes 130°W and 168°W. Its associated grid has a mesh of 0.125° by 0.125°. Note that this grid also encompasses a significant portion of western Canada. The area of the Bering region ranges between latitudes 50° N and 70° N and between longitudes 168° W and 195° W. Its associated grid has a mesh of 0.5° by 0.5°. Note that this grid also encompasses a significant portion of eastern Russia. The velocity model presented in this document for the Alaska region is essentially an upgrade of the Alaskan velocity model encoded in Version 0.1 of TRANS4D. The presented velocity model for the Bering region is new to TRANS4D.

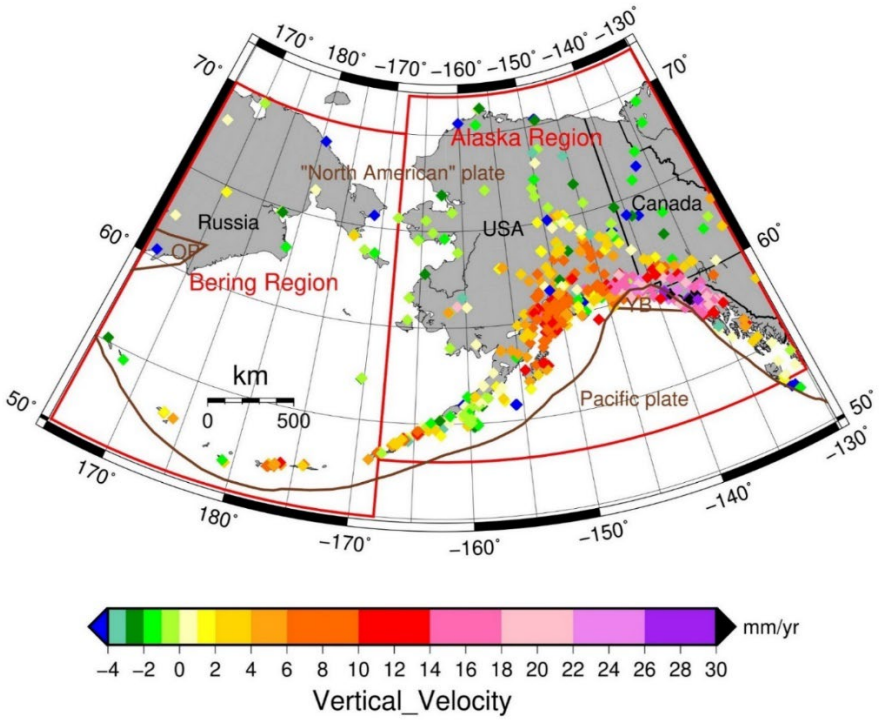

Figure 1. Diamonds identify geodetic stations whose IGS14 vertical velocities each has a standard deviation ≤ 2.0 mm/yr. A diamond's color corresponds to the station's estimated IGS14 vertical velocity. The red spherical rectangles identify the borders of the Alaska region and the Bering region as encoded into TRANS4D. Brown curves correspond to tectonic boundaries. OP denotes the Okhotsk plate, and YB denotes the Yakutat block. The name of the North American plate is enclosed within quotation marks due to some uncertainty about the extent of this plate. The curved string of stations located on an arc in the lower left-hand corner of this figure reside on the Aleutian Islands (175° E to 163 ° W) and on the Alaskan Peninsula (163° W to 154° W).

2. Geodetic Data

The new 3D velocity models for both the Alaska region and the Bering region have been formulated by using velocity vectors derived from geodetic observations. These velocity vectors were obtained from 16 separate data sets provided by multiple institutions and researchers. In many cases, a velocity vector contained in one data set may have been computed from essentially the same geodetic data used to compute a velocity vector contained in another data set. Only eight of the 16 data sets include velocity estimates for geodetic stations located in either the Alaska region or the Bering region. Nevertheless, velocity estimates provided by the other eight data sets help to align the velocities from all 16 data sets to a common reference frame, namely, the IGS14 frame associated with the International Global Navigation Satellite System Service (IGS). Brief descriptions of each of the eight data sets that directly provide velocity estimates for the Alaska region and/or the Bering region follow:

- The IGS data set is based on continuous GNSS data observed between January 2, 1994 and December 30, 2022, at more than 1,500 IGS-affiliated stations distributed around the world [5].

The IGS updates its solution on a weekly basis. These velocities are referred to the IGS14 reference frame.

- A data set currently maintained by Michigan State University for 3D velocities at more than 1,100 geodetic stations mostly located in and around Alaska (some stations have been observed continuously, others in campaign mode), most of which were used by [6]. However, this data set extends into the Russian Far East [7].
- A data set produced by the University of Nevada at Reno (UNR) [8] that provides estimated IGS14-consistent 3D velocities for more than 15,700 continuous GNSS stations distributed around the world. The latest derived velocities are available at [9].
- A data set produced by [10] that provides IGS14-consistent 3D velocities derived from GPS data observed between 1996 and 2017 at approximately 2,393 continuously-operating GPS stations including those in NOAA's National Continuously Operating Reference Station Network (NCN), plus many contained in the IGS-affiliated global network. The adopted NCN velocity estimates may be obtained at [11].
- A data set produced by the Canadian Geodetic Survey at Natural Resources Canada [12]. These data provide 3D velocity estimates at more than 1,000 stations by employing observations ranging from 2011 to 2017. Velocities were computed at continuously-operating GPS stations located in Canada, the northern portions of the USA, all of Greenland, plus a set of globally distributed sites to help relate the resulting velocities--which are expressed in a Canadian-based reference frame--to velocities expressed in alternative global and national reference frames. Velocities were also computed using data from repeat high accuracy campaign surveys in Canada.
- A data set produced by Geodesy Advancing Geosciences and Earthscope (GAGE) which includes IGS14 consistent 3D velocities for more than 3,900 continuous GNSS stations distributed around the world, including those contained in the University NAVSTAR Consortium's (UNAVCO's) Plate Boundary Observatory (PBO) [13]. The GAGE velocities are updated annually with the latest results available at [14].
- A data set produced by the National Aeronautics and Space Administration's (NASA's) Jet Propulsion Laboratory (JPL) which provides IGS14 consistent 3D velocities for more than 2,650 continuous GNSS stations distributed around the world. The latest results are available at [15].
- The Making Earth System data records for Use in Research Environments (MEaSUREs) data set produced jointly by NASA's Jet Propulsion Laboratory and Scripp's Orbit and Permanent Array Center [16]. This data set provides IGS08-consistent velocities for more than 2,900 continuous GPS stations distributed around the world. The MEaSUREs velocities are updated weekly.

Using the combination process described in Appendix A of [1], the derived velocities from the 16 data sets were employed to estimate a single 3D IGS14 velocity for each of approximately 16,475 distinct geodetic stations. Of these stations, approximately 982 reside within the boundary of the Alaska region or within the boundary of the Bering region. The remaining stations span the globe. Velocities at the stations located around the world were included in the combination process to more accurately estimate the seven parameters required for each of the 16 data sets to transform its velocities from its associated reference frame to the IGS14 reference frame. Actually, a set of seven parameters is needed for each of only 15 of the data sets because the velocities of the IGS data set are already referred to IGS14. The seven parameters include three translations rates ($\dot{T}_X, \dot{T}_Y, \dot{T}_Z$), three rotation rates ($\dot{R}_X, \dot{R}_Y, \dot{R}_Z$), and a scale change rate ($\dot{S}$). Here the subscripts *–X, Y, Z*—pertain to the three axes of a traditional right-handed Earth-centered-Earth-fixed (ECEF) Cartesian coordinate system with the *Z*-axis approximating Earth's axis of rotation and the positive *X*-axis piercing Earth's equator near 0° longitude. See [1] for additional information about the employed combination process.

In this document, velocities contained in the 16 data sets are referred to as stage-1 velocities, and the velocity estimates produced via the combination process are referred to as stage-2 velocities. The diamonds appearing in Figure 1 identify the geodetic stations--located in either of the two spherical rectangles of this study—each of whose stage-2 vertical velocity has a standard deviation that is no larger than 2.0 mm/yr. The color of each diamond corresponds to the stage-2 vertical velocity of the corresponding station. In subsequent sections of this document, a two-step process is discussed which employs selected stage-2 velocities to estimate IGS14 velocities at each grid node of the two spherical rectangles. The resulting velocities at these grid nodes are referred to as stage-3 velocities. Stage-3 velocities correspond to the velocities encoded into the TRANS4D software.

The standard deviation assigned to a stage-2 velocity component (north, east, or up) of a geodetic station equals the minimum value of the reported standard deviations, pertaining to this velocity component, among all of the stage-1 velocities at this station with the following restrictions: (1) the standard deviation of a stage-2 horizontal velocity component cannot be smaller than 0.2 mm/yr, and (2) the standard deviation of a stage-2 vertical velocity cannot be smaller than 0.3 mm/yr. These lower bounds are consistent with the results presented in Figure 2 of [10]. The standard deviation of a stage-2 velocity component was assigned in this way because the various stage-1 velocities are based upon very similar sets of geodetic data and thus do not represent independent estimates. Also, it is not uncommon for different institutions to estimate different velocities with different standard deviations at a station, even though they may be using essentially the same data for that station.

3. Modeling Velocities

The employed velocity-modeling process is a two-step procedure that uses stage-2 velocities to estimate stage-3 velocities. This process is discussed in some detail in [3], thus only an outline is presented here. For the first step (called Step A), a preliminary model for the 3D velocity field is specified. This preliminary model may be imported from a previous study. Alternatively, this previous model may be developed by using equations to characterize velocities in terms of relevant parameters. For the second step (called Step B), a residual velocity is calculated for each available stage-2 velocity located in the designated study area by subtracting from each stage-2 velocity its corresponding velocity yielded by the preliminary model. Then the interpolation process, discussed in the following paragraph, is applied to the set of residual velocities to estimate an incremental velocity for each of several designated points located in the study area. For this study, these designated points will be the nodes of a two-dimensional grid spanning the previously specified spherical rectangle. Each of these incremental velocities are then added to its corresponding velocity, as generated via the preliminary model, to produce a stage-3 velocity. Thus, via bilinear interpolation, the resulting set of stage-3 velocities at the specified collection of grid nodes forms the foundation for an updated velocity model for all points located in the designated spherical rectangle.

In this document, the spatial interpolation of the residual velocities is performed one component at a time (north, east, up) using all available residual velocities derived from the stage-2 velocities located within a prespecified distance of the location at which an estimated (residual) velocity is desired. The applied interpolation process is a variation of kriging [17]. In particular, for each component of the residual velocities, a function needs to be estimated which relates the semivariance between two available residual velocities to the distance between their respective locations. For each residual velocity component at a specified location, this function dictates how much each of the available residual velocities contributes to the estimated value of that component. For mathematical details, see [3].

For the interpolation at a given location, a prespecified maximum distance of 50 km from this location was used except when the resulting circular area around this location contained less than seven residual

stage-2 velocities, in which case the prespecified maximum distance was increased to 100 km unless there were no stations located within 100 km of the given location. In the latter case, the new velocity at the location was set equal to its preliminary velocity. These exceptions were required to estimate velocities in several remote areas.

For this study, the employed preliminary velocity model equals the velocity model encoded in Version 0.3 of TRANS4D. Thus, for the Alaska region, the employed preliminary velocity model equals the velocity model for the Alaska region which was described by [1]. However, because the Bering region is new to TRANS4D, previous versions of this software treat the points located in this region to move horizontally as if they resided on the rigid part of the North American plate. In particular, Version 0.3 (the most recent past version) uses the Euler-parameters for the North American plate as estimated by [18] to predict horizontal velocities for points located in the Bering region. Furthermore, Version 0.3 assumes that all points located in the Bering region have a vertical velocity of 0.0 mm/yr. Because the preliminary velocities may be relatively crude, especially in the case of the Bering region, the solution for each of the two regions was iterated twice. That is, the resulting stage-3 estimates for the 3D velocities served to obtain preliminary velocities for a second solution in which the newer residual velocities should be smaller in magnitude than the original residual velocities and then these upgraded velocities served as preliminary velocities to obtain a third solution.

4. Estimated Vertical Velocities

Figure 2 presents a map of the interpolated stage-3 IGS14 vertical velocities found within the adopted study area. Note that such velocities are not shown at places located more than 100 km from any geodetic station included in this study. Also, velocities are not shown at places where the standard deviations for these estimated velocities exceed 2.0 mm/yr. The TRANS4D software, however, will output an IGS14 vertical velocity of 0.0 mm/yr for those points located more than 100 km from any geodetic station involved in this study, and this software will assign a nominal value of 5.0 mm/yr for the standard deviation of the corresponding velocity. Note that TRANS4D may yield a nonzero vertical velocity when it transforms a zero-value IGS14 vertical velocity from IGS14 to its corresponding vertical velocity relative to a different reference frame (an inevitable consequence of frame transformations). Figure 3 presents a map displaying estimated standard deviations for the interpolated stage-3 IGS14 vertical velocities located within the larger land masses.

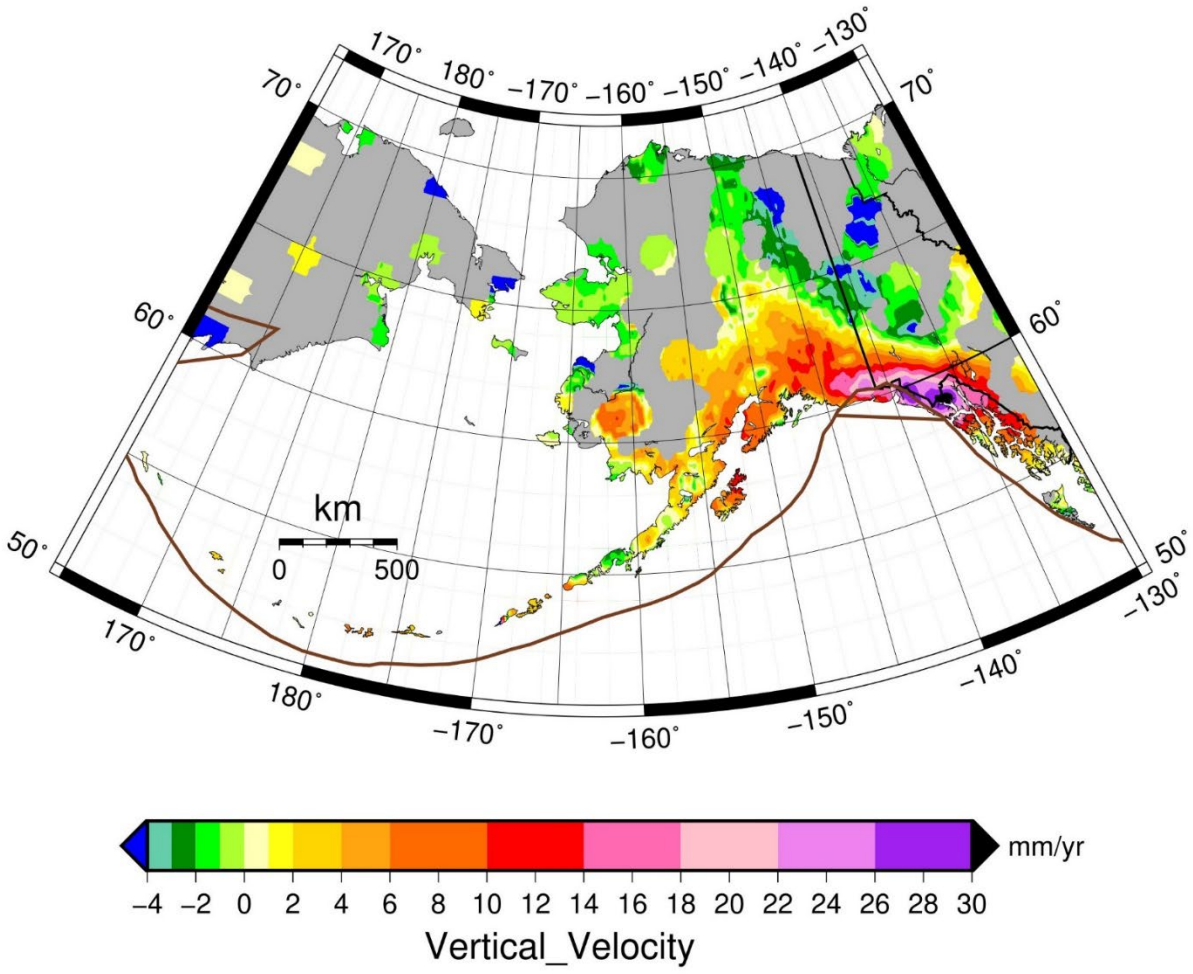

Figure 2. Interpolated stage-3 IGS14 vertical velocities in and around Alaska and the Bering Sea. Gray regions identify areas where the corresponding standard deviations exceed 2.0 mm/yr.

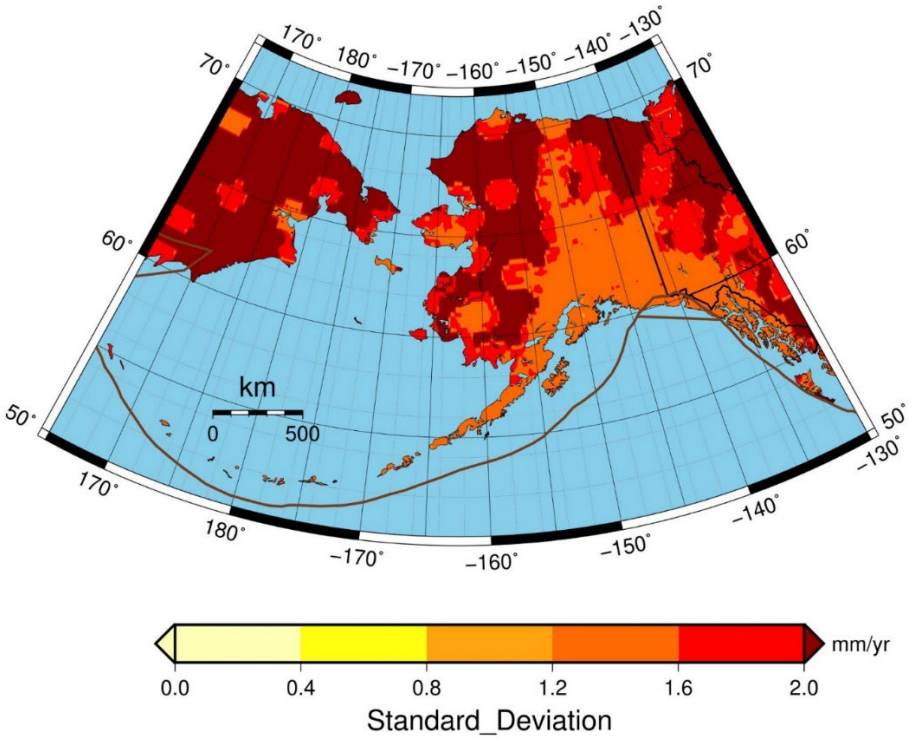

Figure 3. Standard deviations of interpolated stage-3 IGS14 vertical velocities in the vicinity of Alaska and the Bering Sea.

Figure 2 shows that significant uplift is occurring throughout most of the southern part of the Alaska region which resides between longitudes 135° W and 155° W. This uplift may be due in part to the subduction of the Pacific plate and collision of the Yakutat block with the North American plate [6]. This uplift may also be due in part to Glacial Isostatic Adjustment (GIA)—both the GIA associated with the past melting of the ice fields that formed more than 19,000 years ago during the Last Glacial Maximum [19] and the ice fields formed during the Little Ice Age advance that occurred between 1550 AD and 1850 AD [20]. In contrast, pervasive subsidence is occurring in those parts of the Alaska region (including western Canada) which are located north of latitude 65° N and between longitudes 130° W and 168° W. This subsidence is also due in great part to these two sources. On the other hand, little can be inferred from the interpolated velocities shown in Figure 2 regarding the geophysical phenomena that are occurring in the Bering region. This situation is due to the relative sparsity of the available geodetic data that reside there. Nevertheless, when the vertical velocities are viewed in combination with the horizontal velocities, a fuller picture of the geophysical phenomena that occur in the Bering region can be obtained, as is discussed later in this document.

Note that Figure 3 shows the standard deviations for the interpolated stage-3 velocities exceed 1.2 mm/yr almost everywhere within both the Alaska region and the Bering region. Such high standard deviations may be expected due to the sparsity of geodetic stations in many parts of these two regions. However, such relatively large standard deviations also exist near the Pacific coast of Alaska where many monitored geodetic stations reside. These large standard deviations occur in such coastal areas because of the large variability in the observed vertical velocities among closely spaced geodetic stations, as

shown in both Figure 1 and Figure 2. Said differently, the high variability in the vertical velocities among closely spaced geodetic stations greatly limits the accuracy with which vertical velocities can be interpolated, and hence, the interpolated vertical velocities have relatively large standard deviations.

While on the topic of standard deviations, it should be mentioned that maps, like the one presented in Figure 3, were also created for displaying the standard deviations of interpolated east-west velocities and for displaying the standard deviations of interpolated north-south velocities. In each of these two latter cases, the resulting map is essentially indistinguishable from the map shown in Figure 3 for the same two reasons: (1) the sparsity of geodetic stations in the same areas and (2) the large variability among east-west velocities and among north-south velocities in areas where ample horizontal velocities have been observed, such as near the Pacific coast of Alaska.

5. Estimated Horizontal Velocities in the Alaskan Region

According to the theory of plate tectonics, the interior of a plate is generally considered to be rigid, whereas a tectonic plate usually undergoes deformation in the vicinity of those areas where it interacts with one or more other plates. The linear extent of this area of interplate interaction often exceeds 100 km. Moreover, in the area where adjacent plates interact, part of each plate may be partitioned into a collection of tectonic blocks where the interior of each block may be deforming. Often, the border between two adjacent blocks is delineated by a geologic fault. Figure 4 illustrates how the Alaskan region is deforming horizontally whereas Figure 2 illustrates how both the Alaskan region and the Bering region are deforming vertically. Both the horizontal and vertical components of the deformation observed in the Alaska region are in great part due its interaction with both the Pacific plate and the Yakutat block [6] and also in great part due to GIA [19, 20]. To help make the distinction between the deformation due to the interaction among adjacent plates and/or blocks and the deformation due to GIA, the horizontal motion presented in Figure 4 is plotted relative to recent estimates of the Euler-pole parameters for the North American plate which were derived by [18]. In particular, [18] estimated that the North American plate is rotating counter-clockwise at a rate (ω) of 0.1943 ± 0.0009 °/Myr around a pole that pierces Earth's surface at a latitude (ϕ) equal to 5.00 ± 0.06° S and at a longitude (λ) equal to 85.74 ± 0.24° W. These three Euler-pole parameters may be alternatively represented as three rotation rates (ω_X, ω_Y, ω_Z) around poles that respectively correspond to the positive X-axis, the positive Y-axis, and the positive Z-axis of an ECEF Cartesian coordinate system. The relationship between these two representations of Euler-pole parameters is expressed by the following three equations:

$$\omega_X = \omega \bullet \cos\phi \bullet \cos\lambda \quad (1)$$

$$\omega_Y = \omega \bullet \cos\phi \bullet \sin\lambda \quad (2)$$

$$\omega_Z = \omega \bullet \sin\phi \, . \quad (3)$$

As a result, $(\omega_X, \omega_Y, \omega_Z) = (0.2668, -3,3677, -0.2956) \bullet 10^{-9}$ radians/yr. (4)

This alternative representation of the Euler-pole parameters is convenient for converting the IGS14 velocities (V_{Xa} , V_{Ya} , V_{Za}) at a point whose IGS14 positional coordinates are (X_a , Y_a, Z_a) to its equivalent velocity (V_{Xb} , V_{Yb} , V_{Zb}) relative to a "fixed" North American plate via the equations:

$$V_{Xb} = V_{xa} + (\omega_Z)\bullet Y_a \; - \; (\omega_Y)\bullet Z_a \quad (5)$$

$$V_{Yb} = V_{Ya} - (\omega_Z)\bullet X_a \; + (\omega_X)\bullet Z_a \quad (6)$$

$$V_{Zb} = V_{Za} \; + (\omega_Y)\bullet X_a - (\omega_X)\bullet Y_a \quad (7)$$

when ω_X , ω_Y , and ω_Z are each small in magnitude, as is the case for the North American plate.

These parameters should quantify the horizontal motion of the “stable” interior of the North American plate. There are a couple caveats, however. First, the Euler-pole parameters estimated by [18] are relative to IGS08, whereas this report treats these parameters as if they were relative to IGS14. Second, [21] computed horizontal strain rates within an area that includes what many scientists consider to be the “stable” interior of the North American plate (for example, some area located in or near the eastern parts of the USA and Canada), and the authors of [21] found that almost all of this area is undergoing horizontal strain rates that differ statistically from a value of zero strain/yr. It is highly likely that ongoing GIA is the dominant source of these statistically significant strains rates. To address this situation, [18] employed the ICE-6G_D(VM5a) model [19] to remove the horizontal motion due to GIA in eastern North America prior to estimating the values of the Euler-pole parameters for the North American plate. It is highly likely that better GIA models will be forthcoming within a few years whereby the Euler-pole parameters for the North American plate may soon be estimated more accurately.

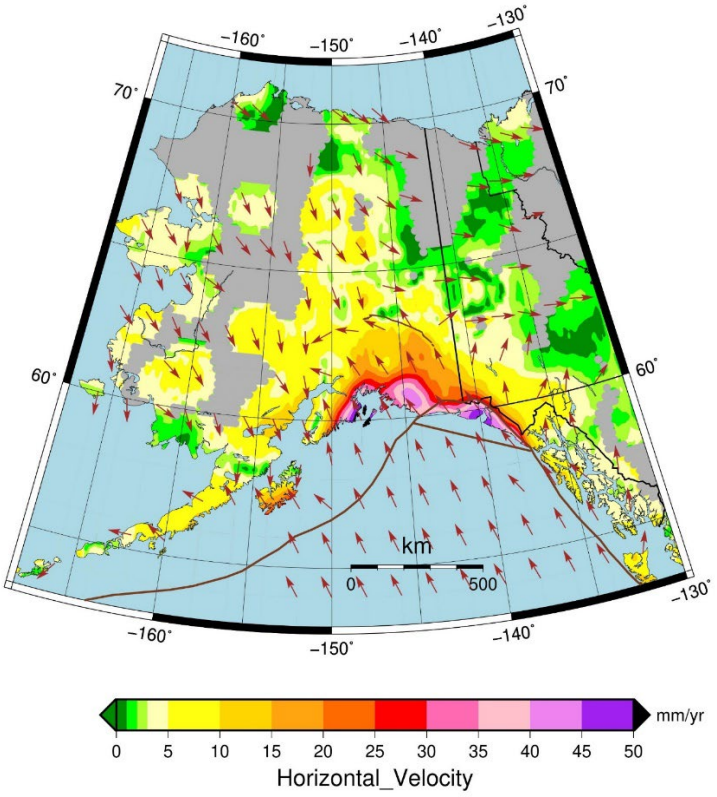

Figure 4. Estimated stage-3 horizontal crustal velocities relative to the “stable” interior of the North American plate as defined by this plate’s Euler-pole parameters as estimated by [18]. The thicker brown curves correspond to tectonic boundaries. The thinner brown line corresponds to the surface trace of that part of the Denali fault that ruptured during the magnitude 7.9 earthquake of 2002. The gray patches identify areas where the standard deviation of the eastward velocity component exceeds 2.0 mm/yr. Otherwise, colors denote the speed and arrows denote the direction for the estimated horizontal velocities.

As displayed in Figure 4, the direction of horizontal motion of the Pacific plate seen in the southeastern corner of this graphic is oriented northwestward, and this direction of motion extends into central Alaska, at least until it reaches the trace of the Denali fault that ruptured during a magnitude 7.9 earthquake that occurred in 2002. On the other hand, the direction of horizontal motion occurring in the northwestern corner of this graphic is oriented essentially southeastward. Thus, the surface trace of the ruptured segment of the Denali fault most likely constitutes part of a boundary between two tectonic blocks.

Another abrupt boundary between these two patterns occurs along a north-south trending line located slightly west of longitude 150°W. This line extends approximately from latitude 63°N to latitude 59°N. The relevance of this north-south trending line will be addressed shortly. Meanwhile, note that [6] provides an extremely detailed description of the horizontal motion occurring in the Alaska region. However, the directions of their estimated velocities differ slightly from the directions displayed in Figure 4, partly because they employed a different set of Euler-pole parameters for the North American plate; namely, they employed the parameters estimated by [22]. It is also important to emphasize that the horizontal motion presented in Figure 4 includes both that motion due to plate tectonics and that motion due to GIA, while the velocities presented by [6] employed models to remove the motion due to GIA and thus their presented velocity field addresses only those velocities due solely to tectonic motion.

6. Estimated Horizontal Velocities in the Vicinity of a Hypothesized Bering Plate

According to a number of studies [23-26], an area located in and around the Bering Sea forms part of a Bering plate; and hence, this area would not be part of the North American plate as is illustrated in Figure 1. However, past studies have disagreed about the spatial extent of the Bering plate, with some including the southern Bering Sea and the Aleutian arc (eg., [23]). [6] showed that once postseismic deformation from the 1964 Alaska earthquake is removed from the observed velocities, the crust of the southern Bering Sea (roughly south of the Kaltag fault) was better interpreted in terms of a series of tectonic slivers moving to the southeast. [6] assigned sites in the Bering Strait region to a Bering Strait block, but they did not consider data from eastern Russia.

To test for the existence and spatial extent of the Bering plate, this study used estimated stage-2 IGS14 horizontal velocities to estimate Euler-pole parameters for the would-be Bering plate and to help locate the stable interior of this plate. As described by [4], a process for estimating Euler-pole parameters involves an iterative search where these parameters are first computed using the IGS14 stage-2 horizontal velocities for a large number of candidate geodetic stations. Then, several of the employed stations--that have rather large horizontal velocities relative to the computed parameters--are eliminated. Then, the process is repeated several times until all of the remaining geodetic stations have horizontal velocities whose magnitudes are each less than 1.0 mm/yr relative to the latest estimates of the Euler-pole parameters. This iterative process identified 20 geodetic stations whose motions are well described by a rigid plate rotation. These 20 sites are listed in Table 1. As shown in Figure 5, these sites span part of the Bering region, including several sites located in eastern Russia and two stations located on St. Lawrence Island. On the Alaska side of the Bering Strait, these sites mostly lie on the Bering Strait Block of [6], although two sites--located to the south of latitude 62°N--are included as well. The estimates for the Euler-pole parameters (relative to IGS14) for this plate may be quantified by three parameters whose estimated values are:

$$(\omega_X , \omega_Y , \omega_Z) = (0.0892, -0.2034, -0.1135)\ ^\circ/\text{Myr} \qquad (8)$$

and whose respective standard deviations have the estimated values

(0.0060, 0.0015, 0.0128) °/Myr. (9)

Here (ω_X , ω_Y , ω_Z) represent counter-clockwise rotation rates around the X-axis, Y-axis, and Z-axis of an ECEF Cartesian coordinate system, and °/Myr denotes degrees per 1,000,000 years. By employing Equations 5, 6, and 7; the three estimated rotations specified in Equation 8 may be used to convert IGS14 horizontal velocities to equivalent horizontal velocities relative to a new reference frame for the Bering plate. This new frame will be referred to as the Bering Terrestrial Reference Frame of 2014 (BETRF14) in this document.

Table 1. Horizontal velocities for the 20 geodetic stations used to estimate Euler-pole parameters for the Bering plate.

Geodetic Station	Latitude	Longitude	IGS14 north velocity	IGS14 east velocity	BETRF14 north velocity	BETRF14 east velocity
	degrees north	degrees east	mm/yr	mm/yr	mm/yr	mm/yr
8756	64.5073	194.5699	-24.79 ± 0.25	-1.54 ± 0.34	-0.45	0.40
AB04	63.6569	189.4326	-23.74 ± 0.20	-0.88 ± 0.20	0.16	-0.69
AB08	60.3848	193.7991	-24.65 ± 0.22	-2.47 ± 0.20	-0.36	0.12
AB09	65.6150	191.9379	-23.63 ± 0.20	-1.18 ± 0.20	0.51	-0.51
AB11	64.5645	194.6265	-24.32 ± 0.20	-1.81 ±0.20	0.03	0.14
AB17	63.8864	199.3053	-24.55 ± 0.20	-4.31 ± 0.20	0.03	-0.42
AC07	65.9613	198.7134	-24.13 ± 0.20	-3.48 ± 0.20	0.43	-0.26
AC31	64.6380	197.7609	-24.55 ± 0.20	-2.83 ± 0.20	-0.03	0.31
AC50	65.5538	195.4334	-23.90 ± 0.20	-2.10 ± 0.20	0.50	-0.07
EGV1	66.3253	180.8812	-22.40 ± 0.37	2.98 ± 0.45	0.33	-0.67
EGVK	66.3220	180.8816	-22.73 ± 0.24	3.17 ± 0.29	0.00	-0.48
ETID	64.6165	197.7479	-24.45 ± 0.27	-2.23 ± 0.34	0.07	0.91
GAMB	63.7745	188.2680	-23.46 ± 0.22	-0.06 ± 0.28	0.31	-0.33
HPBB	61.5274	193.8483	-24.85 ± 0.20	-1.67 ± 0.27	-0.56	0.68
LAV1	65.6167	188.8976	-23.20 ± 0.33	1.05 ± 0.39	0.64	0.56
MELS	64.9223	196.3077	-24.47 ± 0.20	-2.58 ± 0.20	-0.02	-0.07
MRKV	64.6828	170.4042	-20.76 ± 0.23	7.27 ± 0.26	-0.15	0.48
NOME	64.5627	194.6288	-24.97 ± 0.20	-1.81 ± 0.22	-0.62	0.14
OMEB	64.5129	194.5664	-24.38 ± 0.20	-2.02 ± 0.25	-0.04	-0.09
OTZ1	66.8873	197.3886	-24.85 ± 0.20	-1.85 ± 0.20	-0.35	0.65

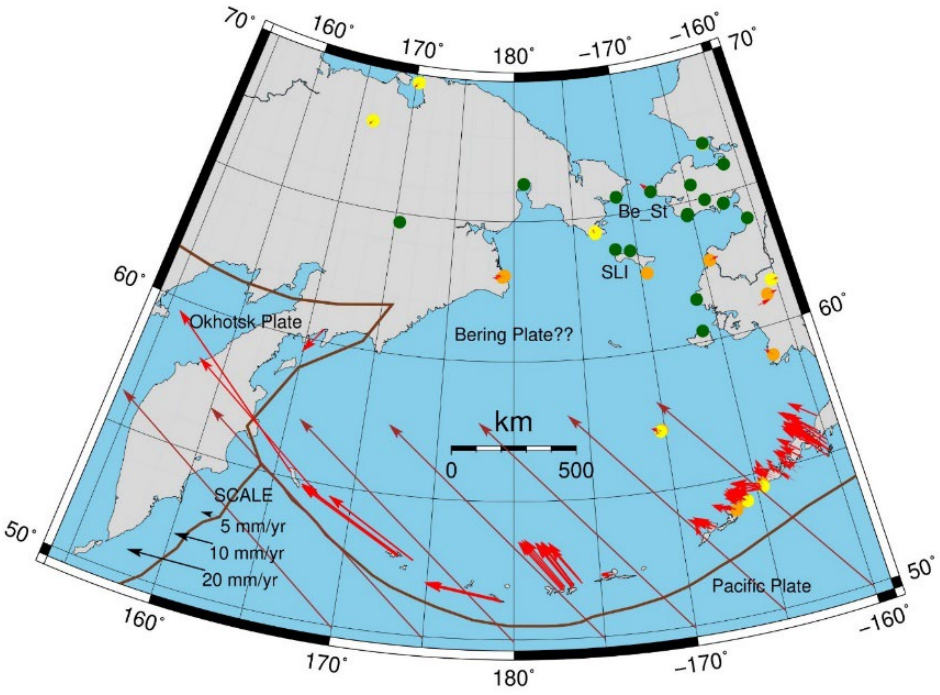

Figure 5. Red vectors represent stage-2 horizontal velocities in a reference frame based on estimated Euler-pole parameters for the hypothesized Bering plate. Green dots identify the locations of geodetic stations whose stage-2 horizontal velocities have magnitudes less than 1 mm/yr relative to this reference frame. (Correspondingly, yellow dots identify stations whose horizontal velocities have magnitudes between 1and 2 mm/yr, and orange dots identify stations whose horizontal velocities have magnitudes between 2 and 3 mm/yr.) Brown vectors represent the predicted motion of the Pacific plate relative to this reference frame for several locations at a latitude of 50° N and under the assumption that the Pacific plate is not deforming at these locations. SLI = Saint Lawrence Island, and Be_St = Bering Strait.

The values in Equation 8 are equivalent to a counter-clockwise rotation rate of 0.2494 °/Myr about a pole that pierces the Earth's surface at a latitude of 27.07°S and at a longitude of 66.32°W. By way of contrast, the Euler-pole parameters derived by [18] for the North American plate are equivalent to a counter-clockwise rotation rate of 0.1943 °/Myr about a pole that pierces the Earth's surface at a latitude of 5.00°S and at a longitude of 85.47°W.

In Figure 5, green dots identify the 20 geodetic stations that may be considered to reside within the "rigid" interior of the hypothesized Bering plate. Note that five of these 20 stations are located so near to other stations that only 15 green dots can be visually detected in Figure 5, but all 20 stations are listed in Table 1. Also note that three of the green dots are located in eastern Russia. Moreover, note that Figure 5 displays no locations, with velocities exceeding 5 mm/yr, which reside on the would-be Bering plate except in the vicinity of the Alaskan Peninsula or in the vicinity of the Aleutian Islands. The high velocities in these latter two areas may be attributed to their proximity to the interplate boundary that separates the hypothesized Bering plate from the Pacific plate, as illustrated in Figure 5. The brown vectors displayed in Figure 5 represent the predicted velocities that would occur at several locations

under the assumption that these locations reside within the rigid interior of the Pacific plate. The orientation and magnitudes of these brown vectors indicate how the subduction of the Pacific plate beneath the Bering plate would cause the Bering plate to deform in the vicinity of the Alaskan Peninsula and the Aleutian Islands. Otherwise, Figure 5 does not reveal much evidence about the extent of the Bering plate because of the small number of horizontal velocities that have been accurately determined within the geographic extent of this figure, although it is clear that the Alaska Peninsula and the Aleutian Islands themselves move relative to the Bering plate.

7. Searching for an Interplate Boundary

According to Figure 5, several of the geodetic stations, which are considered to be located in the stable interior of the hypothesized Bering plate, also reside east of longitude 168° W. Hence, these stations reside in the Alaska region of this study. Also, Figure 4 reveals that the part of the Alaska region located west of 150° W and north of latitude 60° N is moving in a southeasterly direction, in some cases with speeds exceeding 5 mm/yr. Could this motion support the case for the existence of a Bering plate? To address this question, Figure 6 has been created to illustrate the horizontal velocity field for the Alaska region relative to the newly estimated Euler-pole parameters of the hypothesized Bering plate, rather than relative to the Euler-pole parameters for the North American plate.

In this study, it is proposed that part of the boundary between the proposed Bering plate and the North American plate resides as depicted by the string of dark blue dashes presented in Figure 6. In particular, this boundary includes part of the east-west trending Kobuk fault with the Bering plate located to the south of this fault. Around longitude 146°W, the proposed interplate boundary takes a sharp turn southward and trends along a sinuous narrow path (colored pale yellow in Figure 6) where horizontal velocities range from 3 to 5 mm/yr in magnitude. The narrowness of this path indicates a significant spatial variation among the local horizontal velocities oriented perpendicular to this path (as would be the case in an interplate boundary). This path then takes a sharp turn toward the west as it follows along the Denali fault which ruptured significantly during an M 7.9 earthquake that occurred in 2002. Just west of longitude 150°W, the path turns southward again until it encounters an even narrower green-colored path that continues essentially southward along the west coast of the Kenai peninsula. South of this peninsula, this proposed interplate boundary presumably progresses southward into the Pacific Ocean until it terminates somewhere along the northern boundary of the Pacific tectonic plate at a location east of Kodiak Island. This proposed interplate boundary elaborates on a somewhat similar boundary proposed by [27]. See their Figure 17.

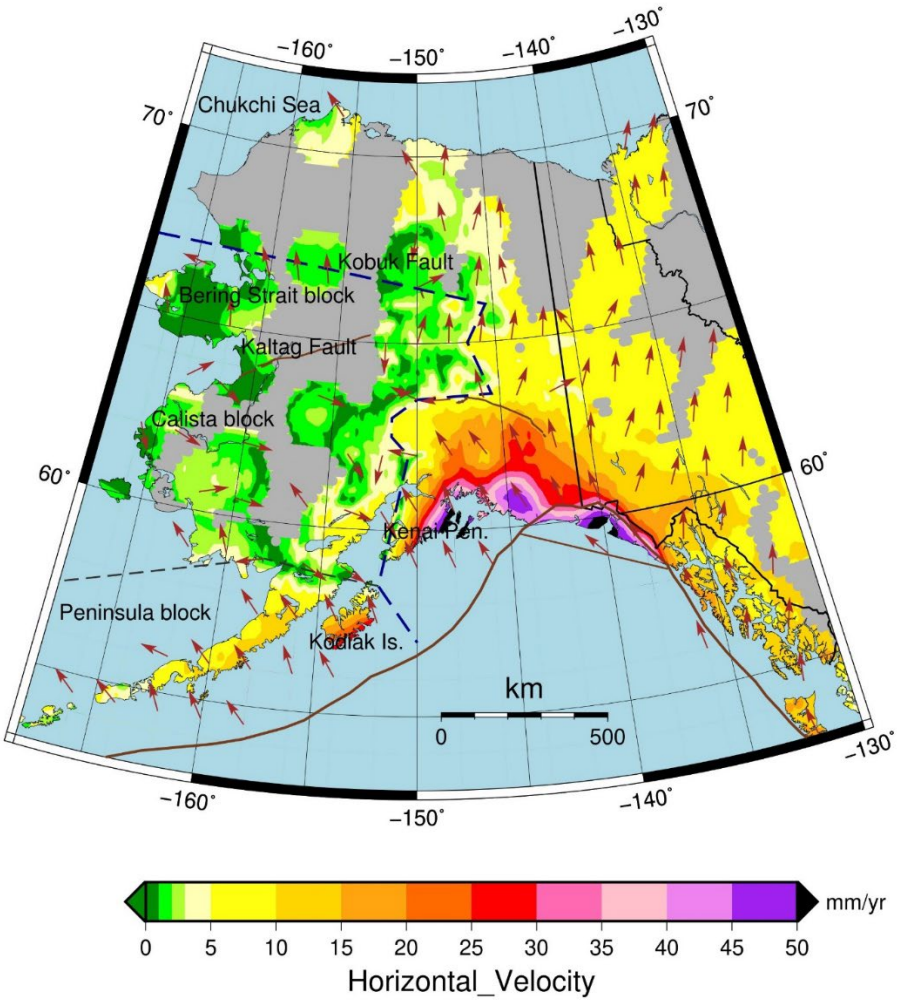

Figure 6. Estimated stage-3 horizontal velocities relative to the newly computed Euler-pole parameters for the hypothesized Bering plate. The dark blue dashes represent a proposed part of the boundary between the Bering plate and the North American plate. The light gray patches identify areas where the standard deviations for the eastward velocity components exceed 2.0 mm/yr. Otherwise, colors denote the speed and arrows denote the direction of the estimated velocities.

The horizontal velocity vectors presented in Figure 6 also suggest that part of at least three tectonic blocks reside on the Bering plate. In this report, these blocks are referred to as the Bering Strait block, the Calista block, and the Peninsula block. The Bering Strait block is located at the northeastern most extreme of the proposed Bering plate as is displayed in Figure 6. The Calista block is located immediately south of the Bering Strait block, and the Peninsula block is located immediately south of the Calista block. This delineation of blocks within the plate, if correct, is consistent with the notion that the Kaltag fault forms most of the proposed boundary between the Bering Strait block and the Calista block as is shown in Figure 6. The proposed boundary between the Calista block and the Peninsula block

is displayed as a black dashed line in Figure 6. The Peninsula block is bounded to its south and east by the Pacific plate. It is also possible that the Peninsula block could be a tectonic sliver that may not belong to any tectonic plate.

Although the Bering Strait block contains several geodetic stations that reside in the stable interior of the proposed Bering plate, parts of this block experience horizontal velocities slightly exceeding 3 mm/yr relative to the reference frame defined by the Euler-pole parameters of the Bering plate. These higher velocities may be due to local deformation and/or to interactions with bordering tectonic blocks (including those tectonic blocks residing on the North American plate).

The Calista block experiences eastward oriented horizontal velocities. Its velocities that have the largest magnitudes occur near to where this block abuts the North American plate, especially south of latitude 64° N. Part of the Calista block's eastern boundary is near the west coast of the Kenai Peninsula. As shown in Figure 6, the part of the Kenai Peninsula located east of the proposed boundary between the Bering plate and the North American plate is undergoing extreme east-west oriented horizontal contraction.

The proposed boundary between the Calista block and the Peninsula block actually resides along an essentially east-west trending path located partly in mainland Alaska and partly in the channel separating mainland Alaska from the Alaskan peninsular. In Figure 6, a dashed line approximates the proposed boundary between the Peninsula block and the Calista block. It is proposed that Kodiak Island also resides on the Peninsula block. Velocities on this island range in magnitude from 5 mm/yr to 25 mm/yr because of this island's proximity to the Pacific plate. As previously mentioned, the southern boundary of the Peninsula block coincides with this block's boundary with the Pacific plate.

8. Summary

This document introduces Version 0.4 of the TRANS4D software. This version provides an updated 3D velocity model for most of Alaska and for parts of northwestern Canada. It also introduces a 3D velocity model for parts of the Bering Sea, the Aleutian Islands, and eastern Russia. While these velocity models are expressed relative to the IGS14 reference frame, TRANS4D is capable of transforming these velocities to several other popular reference frames. This documents also presents evidence for the existence of a Bering plate. In particular, 20 geodetic stations were identified that are thought to reside in the "stable" interior of this plate. Using these 20 stations, values for the Euler-pole parameters for the hypothesized Bering plate were estimated (relative to IGS14). Moreover, estimated horizontal velocities computed at several geodetic stations located in western Alaska provide evidence for the existence of part of an interplate boundary between the North American plate and the hypothesize Bering plate.

Acknowledgements

The authors thank the many people and institutions that were involved in collecting and/or processing the geodetic data included in this study. The authors also thank Jarir Saleh who developed much of the software encoded into TRANS4D, and they thank Tony Lowry, Richard Bennett, and Phillip McFarland for suggestions that improved the presentation of this paper significantly. The paper was supported in part by the National Geodetic Survey. The figures have been drawn using Generic Mapping Tools [28]. Version 0.4 of the TRANS4D software and this software's documentation may be obtained by submitting a request via email to rssnay@aol.com.

References

1. Snay RA, Freymueller JT, Craymer MR, Pearson CF, Saleh J. Modeling 3-D crustal velocities in the United States and Canada. J Geophys Res Solid Earth 2016;121(7):5365-88. http://doi.org/10.1002/2016JB012884

2. International Earth Rotation and Reference System Service. ITRF2014. Accessed August 26, 2022. https://itrf.ign.fr/en/solutions/ITRF2020

3. Snay RA, Saleh J, Pearson CF. Improving TRANS4D's model for vertical crustal velocities in Western CONUS. J Applied Geodesy 2018;12(3):209-27. https://doi.org/10.1515/jag-2018-0010

4. Snay RA, Saleh J, Dennis M, DeMets C, Mora-Páez H. Expanding TRANS4D's scope to include 3D crustal velocity estimates for a neighborhood of the Caribbean plate. J Surv Eng 2021;147(4). https://doi.org/10.1061/(ASCE)SU.1943-5428.0000377

5. National Aeronautics and Space Administration/Goddard Space Flight Center, CDDIS: NASA's Archive of Space Geodesy Data. Accessed November 15, 2022. https://cddis.nasa.gov/archive/gnss/products/2130/

6. Elliott J, Freymueller JT. A block model of present-day kinematics of Alaska and western Canada. J Geophys Res Solid Earth 2020;125(7). https://doi.org/10.1029/2019JB018378

7. Freymueller JT. personal communication, 2020.

8. Blewitt G, Hammond WC, Kreemer C. Harnessing the GPS data explosion for interdisciplinary science. *Eos*, 2018. Accessed November 15, 2022. https://doi.org/10.1029/2018EO104623

9. University of Nevada Reno, Website of Nevada Geodetic Laboratory. Accessed November 15, 2022. http://geodesy.unr.edu

10. Saleh J, Yoon S, Choi K, Sun L, Snay R, McFarland P, Williams S, Haw D, Coloma, F. 1996-2017 GPS position time series, velocities and quality measures for the CORS network. J Applied Geodesy 2021;15:105-15.

11. National Geodetic Survey. Table of ITRF2014 GNSS coordinates. Accessed November 15, 2022. https://noaa-cors-pds.s3.amazonaws.com/coord/coord_14/itrf2014_geo.comp.txt

12. Robin CMI, Craymer M, Ferland R, James TS, Lapelle E, Piraszewski M, Zhao Y. NAD83v70VG: A new national crustal motion model for Canada. *Geomatics Canada*, Open File 0062, 1. zip file. 2020. https://doi.org/10.4095/327592

13. Herring TA, Melbourne TI, Murray MH, Floyd, MA, Szeliga WM, King RW, Phillips DA, Puskas CM, Santillan M, Wang L. Plate Boundary Observatory and related networks: GPS data analysis methods and geodetic products. Rev Geophys 2016;54(4):759-801. https://doi.org/10.1002/2016RG000529

14. University Navstar Consortium, GPS/GNSS data. *Plate Boundary Observatory*. Accessed November 15, 2022. https://data.unavco.org/archive/gnss/products/velocity/cwu.final_igs14.vel

15. National Aeronautics and Space Administration/Jet Propulsion Laboratory. GNSS science data: Table 2. *Jet Propulsion Laboratory at the California Institute of Technology*. Accessed November 15, 2022. https://sideshow.jpl.nasa.gov/post/tables/table2.html

16. Bock Y, Moore AW, Argus DF, Fang P, Jiang S, Kedar S, Knox, SA, Liu Z, Sullivan A. Extended Solid Earth Science ESDR System (ES3): Algorithm Theoretical Basis Document: Chapter 4.2. http://garner.ucsd.edu/pub/measuresESESES_products/ATBD/ESESES-ATBD.pdf (username:anonymous; password: your email address) Accessed November 10, 2022.

17. Goovaerts P. *Geostatistics for Natural Resources Evaluation.* Oxford, UK: Oxford University Press, 1997.

18. Ding K, Freymueller JT, He P, Wang Q, Xu, C. Glacial isostatic adjustment, intraplate strain, and relative sea level changes in eastern United States. J Geophys Res Solid Earth 2019;124:6056- 71. https://doi.org/10.1029/2018JB017060

19. Peltier WR, Argus DF, Drummond R. Comment on 'An Assessment of the ICE-6G_C (VM5a) glacial isostatic adjustment model' by Purcell et al. J Geophys Res Solid Earth 2018;123:2019-28. https://doi.org/10.1002/2016JB013844

20. Hu Y, Freymueller JT. Geodetic observation of time-variable glacial isostatic adjustment in Southeast Alaska and its implications for Earth rheology. J Geophys Res Solid Earth 2019;147:9870-89. https://doi.org/10.1029/2018JB017028

21. Kreemer C, Hammond WC, Blewitt G. A robust estimation of the 3-D intraplate deformation of the North American plate from GPS. J Geophys Res Solid Earth 2018;123. https://doi.org/10.1029/2017JB015257

22. Argus DF, Gordon RG, Heflin MR, Ma C, Eanes RI, Willis P, et al. The angular velocities of the plates and the velocity of Earth's center from space geodesy. Geophysical Journal International 2010;180(3):913-60.

23. Cross RS, Freymueller JT. Evidence for the implication of a Bering plate based on geodetic measurements from the Aleutians and western Alaska. J Geophys Res Solid Earth 2008;113,B07405. https://doi.org/10.1029/2007JB005136

24. Fujita K, Mackey KG, McCaleb RC, Cunbina LV, Kkovalev VN, Imaev, VS, Smirnov VN. Seismicity of Chukotka, northeastern Russia. in *Tectonic Evolution of the Bering Shelf-Chukchi Sea-Arctic Margin and Adjacent Landmasses.* Geol Soc Am Spec Pap Ser, 2002;360:259-72 edited by E. L. Miller, A. Grantz, and S. L. Kemper, Geol Soc of Am, Boulder, Colo.

25. Lander, AV, Bukchin BG, Kiryushin AV, Droznin DV. The tectonic environment and source parameters of the Khailino, Koryakiya earthquake of March 8, 1991: Does a Beringia plate exist? Comput Seismol Geodyn 1996;3:80-96.

26. Mackay KG, Fujita G, Gunbina LV, Kolalev, VN, Imaev VS, Zozmin BM, Imaeva IP. Seismicity of the Bering Strait region: Evidence for a Bering block. *Geology,* 1997;25:979-82. https://doi.org/10.1130/0091-7613(1997)025<0979:SOTBSR>2.3.CO;2

27. Freymueller JT, Woodward H, Cohen SC, Cross R, Elliott J, Larsen CF, Hreinsdóttir S, Zweck C. Active deformation processes in Alaska, based of 15 years of GPS measurement. Active Tectonics and Seismic Potential of Alaska. Geophysical Monograph Series 179, 2008. https://doi.org/10.1029/179GM02

28. Wessel P, Smith WHF. New, improved version of generic mapping tools released. *EOS Trans. Am. Geophysical Union* 1998;79(47):579. https://doi.org/10.1029/98EO00426